

The OIV 1407.3Å/1401.1Å emission-line ratio in a plasma

Nabil Ben Nessib

Department of Physics and Astronomy, College of Science, King Saud University. PO Box 2455, Riyadh 11451, Saudi Arabia.

Norah Alonizan

Department of Physics and Astronomy, College of Science, King Saud University. PO Box 2455, Riyadh 11451, Saudi Arabia.

Rabia Qindeel

Department of Physics and Astronomy, College of Science, King Saud University. PO Box 2455, Riyadh 11451, Saudi Arabia.

Sylvie Sahal-Bréchet

Laboratoire d'Étude du Rayonnement et de la Matière en Astrophysique, Observatoire de Paris, UMR CNRS 8112, UPMC, 5 Place Jules Janssen, 92195 Meudon Cedex, France.

Milan S. Dimitrijević*

*Astronomical Observatory, Volgina 7, 11060 Belgrade, Serbia.
Laboratoire d'Étude du Rayonnement et de la Matière en Astrophysique, Observatoire de Paris, UMR CNRS 8112, UPMC, 5 Place Jules Janssen, 92195 Meudon Cedex, France.*

arXiv:1311.1054v1 [astro-ph.SR] 5 Nov 2013

Abstract

Line ratio of O IV 1407.3 Å/1401.1 Å is calculated using mostly our own atomic and collisional data.

Energy levels and oscillator strengths needed for this calculation have been calculated using a Hartree-Fock relativistic (HFR) approach. The electron collision strengths introduced in the statistic equilibrium equations are fitted by Line ratio of O IV 1407.3 Å/1401.1 Å is calculated using mostly our own atomic and collisional data.

Energy levels and oscillator strengths needed for this calculation have been calculated using a Hartree-Fock relativistic (HFR) approach. The electron collision strengths introduced in the statistic equilibrium equations are fitted by polynomials for different energies. Comparison has also been made with available theoretical results.

The provided line ratio has been obtained for a set of electron densities from 10^8 cm^{-3} to 10^{13} cm^{-3} and for a fixed temperature of 50 000 K.

Keywords: atomic data; atomic processes; line ratio

1. Introduction

Triply charged oxygen ion (O IV) belongs to the boron isoelectronic sequence, its ground state configuration is $2s^2 2p^2 P^o$. The boron like ions are widely observed in a variety of astrophysical plasmas. Many researchers have been done a lot of calculations for many parameters of O IV due to its importance in astrophysical plasma. Aggarwal and Keenan (2008) calculated energy levels, radiative rates (A values) and excitation rates or equivalently the

effective collision strengths (γ) which are obtained from the electron impact collision strength (Ω). Feldman et al. (1997) presented a solar coronal spectrum recorded by the extreme UV spectrometer SUMER on the Solar and Heliospheric Observatory. The detected O IV lines covered the wavelength range 500 - 1610 Å. The studied range contains the $2s^2 2p^2 P^o - 2s 2p^2 ^4P$ intercombination transitions. Harper et al. (1999) obtained a high signal-to-noise ratio spectra of RR Tel at medium resolution with the Goddard High-Resolution Spectrograph (GHRS) on the Hubble Space Telescope (HST) to test available atomic data for the intercombination transitions in O IV (multiplet: UV 0.01). Blair et al. (1991) observed the far-ultraviolet spectrum of the Cygnus Loop supernova remnant using the Hopkins Ultraviolet Telescope aboard

*Corresponding author

Email addresses: nbnessib@ksu.edu.sa (Nabil Ben Nessib), nalonizan@ksu.edu.sa (Norah Alonizan), rqindeel@ksu.edu.sa (Rabia Qindeel), Sylvie.Sahal-Bréchet@obspm.fr (Sylvie Sahal-Bréchet), mdimitrijevic@aob.bg.ac.rs (Milan S. Dimitrijević)

the Astro-1 space shuttle. Similarly, Redfield et al. (2002) have been detected lines of O IV in late-type stars within the wavelength range of 910-1180 Å. Sturm et al. (2002) studied emission lines of O IV in IR range from active galactic nuclei and Pagano et al. (2000) observed them in the solar transition region. Keenan et al. (2009) generated theoretical UV and extreme-UV emission line ratio for O IV and presented their strong versatility for diagnostics of electron temperature and electron density for astrophysical plasmas. Extreme-ultraviolet lines emission arising from radiative transition probabilities and electron collision cross-sections in B-like ions were calculated by Flower and Nussbaumer (1975).

Using semiclassical approach, Dimitrijević and Sahal-Bréchet (1995) calculated electron-, proton-, and He III-impact line widths and shifts for 5 multiplets of O IV. The widths, shifts and fitting coefficients data are in the database STARK-B (Sahal-Bréchet et al., 2012).

Recently, Olluri et al. (2013) studied the non-equilibrium ionization effects on the line ratio of O IV.

In this work, we will study the influence of the atomic data on the emission line ratio I(1407.1 Å)/I(1401.1 Å).

2. Atomic Data

In this work, energy levels and oscillator strengths are calculated with the Hartree-Fock relativistic (HFR) approach using Cowan code (Cowan, 1981) and an atomic model including the 13-configurations: 2s² 2p, 2s 2p², 2p³, 2s² 3s, 2s² 3p, 2s² 3d, 2s² 4s, 2s² 4p, 2s² 4d, 2s² 4f, 2s 2p 3s, 2s 2p 3p and 2s 2p 3d.

The obtained energy level data are compared in Table 1 with those of NIST (Kramida et al., 2012), GRASP2 (Aggarwal and Keenan, 2008) (using 219 levels) and MCHF (Tayal, 2006).

The spontaneous emission radiative rate (the so-called Einstein's A-coefficient), A_{ji} is related with the absorption oscillator strength f_{ij} for the transition $i \rightarrow j$ by the standard relation:

$$A_{ji}(\text{a.u.}) = \frac{1}{2} \alpha^3 \frac{g_i}{g_j} E_{ji}^2 f_{ij} \quad (1)$$

where E_{ji} is the transition energy between states i and j in Rydberg units, α is the fine structure constant and g_i and g_j are the statistical weight factors of the initial and final states respectively.

The transition probability in s⁻¹ is then:

$$A_{ji}(\text{s}^{-1}) = \frac{A_{ji}(\text{a.u.})}{\tau_0} \quad (2)$$

with $\tau_0 = 2.4191 \times 10^{-17}$ is the atomic unit of time.

In Table 2, we have compared our values of $\log(g_i f_{ij})$ and transition probability $A_{ji}(\text{s}^{-1})$ with the values taken from NIST database (Kramida et al., 2012) and results from Galavís, Mendoza and Zeippen (1998), Flower and Nussbaumer (1975) and Tayal (2006). Observed wavelengths are from Bromander (1969).

3. Collisional data

The excitation rate coefficient in cm³s⁻¹ can be expressed by the effective collision strength as:

$$C_{ij} = \frac{8.629 \times 10^{-6}}{g_i T^{1/2}} \gamma_{ij}(T) \exp\left(-\frac{E_j - E_i}{kT}\right) \quad (3)$$

where $\gamma_{ij}(T)$ is the effective collision strength related to the collision strength Ω_{ij} by:

$$\gamma_{ij}(T) = \int_0^\infty \Omega_{ij} \exp\left(-\frac{E_j}{kT}\right) d\left(\frac{E_j}{kT}\right) \quad (4)$$

The excitation rate coefficient C_{ij} can also be written as a function of the cross-section:

$$C_{ij} = N_e \int_{v_0}^\infty v \sigma_{ij}(v) f(v) dv \quad (5)$$

where v_0 is the threshold velocity and $f(v)$ is the Maxwellian velocity distribution function for electrons.

The semiclassical cross-section $\sigma_{ij}(v)$ can be expressed by an integral over the impact parameter ρ of the transition probability $P_{ij}(\rho, v)$ as

$$\sigma_{ij}(v) = \frac{1}{2} \pi R_1^2 + \int_{R_1}^{R_D} 2\pi \rho d\rho P_{ij}(\rho, v). \quad (6)$$

R_D is the Debye radius and R_1 is the minimum cut-off radius (see Sahal-Bréchet (1969), and Seaton (1962) for neutrals).

4. Line ratio

In a steady state regime, we can write that:

$$\begin{aligned} \frac{dN_i}{dt} &= \sum_{j \neq i, j > i} N_j (C_{ji} + A_{ji}) + \sum_{j \neq i, j < i} N_j C_{ji} \\ &\quad - N_i \left[\sum_{j \neq i, i < j} C_{ij} + \sum_{j \neq i, i > j} (C_{ij} + A_{ij}) \right] \\ &= 0, \end{aligned} \quad (7)$$

where N_i is the number of ions per unit of volume for the energy level i , C_{ij} is the electron collisional rate for transferring ions from level i to level j , and C_{ji} is the collisional rate for transferring ions from level j to level i . In fact, since the local incident radiation is very weak, absorption and induced emission rates are completely negligible compared to collisional rates. So, for transferring ions from level i to level j (or from level j to level i) by radiative processes, only spontaneous emission rates A_{ij} (or A_{ji}) are to be taken into account.

Solving the above set of equations, we obtain the relative populations N_i/N_j for any two levels. The normalization is obtained by the constraint $\sum_i N_i = N_{ion}$, where N_{ion} is the ion density per unit volume.

The local emissivity in the line studied (in units of energy, per unit of volume, per unit of time, and per steradian) for a transition from state j to state i is given by:

$$\varepsilon_{ji} = \frac{h\nu}{4\pi} A_{ji} N_j \quad (8)$$

where h is the Planck constant, and ν the frequency of the transition.

In “mode 1” of [Dufton \(1977\)](#), the observed intensity ratio of two lines is equal to the relevant line emissivity ratio. This is currently assumed in UV coronal studies, and justified when the two lines are formed in the same region of the plasma, and in addition if the emissivities vary slowly in the regions of emission. As [Keenan et al. \(2009\)](#), we will assume that it is the case for the considered O IV lines.

[Keenan et al. \(2009\)](#) studied the line ratio $I(1407.3 \text{ \AA})/I(1401.1 \text{ \AA})$ versus electron density for constant electron temperatures. They used the [Kramida et al. \(2012\)](#) energy values in their calculations. The radiative transition probabilities are taken from different sources cited in their paper and from [Aggarwal and Keenan \(2008\)](#) for the excitation rates.

In our present work, we have used our own calculated energies and oscillator strengths (HFR calculations) that give more self-consistent data. For the collision strengths, we have interpolated linearly the 3 collision strengths given by [Flower and Nussbaumer \(1975\)](#) for the energies 2.8, 4.2 and 5.6 Ry.

Then our atomic energy levels, oscillator strengths and interpolation of the collision strengths have been introduced in the statistical equilibrium code of [Dufton \(1977\)](#) that we have modified to give the intensities calculated both as photons emitted and as energy emitted versus electron density for a given electron temperature.

We have not taken into account the collisions with protons. In fact, our purpose is to study the effect on the behavior of the line ratio using different atomic data from different sources.

Putting different energy levels from different sources have not changed the behavior of the curve but when different oscillator strengths have been used, there is a change. [Figure 5](#) shows the line ratio that we obtain when using the oscillator strengths from [Galavís, Mendoza and Zeippen \(1998\)](#) (solid curve) and when putting our HFR data (dashed curve). The difference is increasing with the electron density to reach 14% for $\log(Ne) = 13$.

5. Conclusion

We generally used our own energy levels and oscillator strengths for calculating Stark widths and shifts of spectral

lines in our previous articles. In the present work, we have introduced cross sections, which are a part of the Stark impact width in the statistical equilibrium in a plasma to determine line ratio that can be an important diagnostic for studying plasma. We have tested the influence of using different sources of atomic and collisional data. We have used a powerful method to calculate the line ratio $I(1407.3 \text{ \AA})/I(1401.1 \text{ \AA})$ by introducing homogenous atomic and collisional data that are mostly calculated by us.

Tests for other lines and for other ions will be done as well as the study of the influence of different parameters (atomic collisional data and parameters of the plasma).

Acknowledgments

This project was supported by King Saud University, Deanship of Scientific Research, College of Science Research Center. The support of Ministry of Education, Science and Technological Development of Republic of Serbia through projects 176002 and III44002 is acknowledged. The support of the ‘Programme National de Physique Stellaire’ (PNPS, INSU-CNRS) and of the LABEX Plas@Par (UPMC, PRES Sorbonne Universities, Paris, France) are also acknowledged.

References

- Aggarwal, K. M. and Keenan, F. P., Energy levels, radiative rates and excitation rates for transitions in O IV, *A&A*, 486, 1053-1067, 2008.
- Blair, W. P., Long, K. S., Vancura, O., et al., Discovery of a fast radiative shock wave in the Cygnus Loop using the Hopkins Ultraviolet Telescope, *ApJ*, 379, L33-L36, 1991.
- Bromander, J. *Arkiv Fysik*, 40, 257, 1969.
- Cowan, R. D., 1981, *The Theory of Atomic Structure and Spectra*, University of California Press, Berkeley, USA
- Dimitrijević, M. S. and Sahal-Bréchet, S., Stark broadening of spectral lines of multicharged ions of astrophysical interest, *A&AS*, 109, 551-552, 1995.
- Dufton, P. L., A program to calculate coronal emission line strength, *Comput. Phys. Commun.*, 13, 25-38, 1977.
- Feldman, U., Behring, W. E., Curdt, W., et al., A coronal spectrum in the 500-1610 Å wavelength range recorded at a height of 21,000 kilometers above the west solar LIMB by the summer instrument on solar and Heliospheric observatory, *ApJS*, 113, 195-219, 1997.
- Flower, D. R., and Nussbaumer, H., On the extreme ultraviolet solar emission of B-like ions: O IV, *A&A*, 45, 145-150, 1975.
- Galavís, M. E., Mendoza, C. and Zeippen, C. J., Atomic data from iron project, *A&AS*, 131, 499-522, 1998.
- Harper, G. M., Jordan, C., Judge, P. G., et al., Lines of O IV and S IV in the Goddard High-Resolution Spectrograph spectrum of RR Tel: Constraints on atomic data, *MNRAS*, 303, L41-L46, 1999.
- Keenan, F. P., Crockett, P. J., Aggarwal, K. M., Jess, D. B., and Mathioudakis, M., Ultraviolet and extreme-ultraviolet line ratio diagnostics for O IV, *A&A*, 495, 359-362, 2009.
- Olluri, K., Gudiksen, B. V., Hansteen, V. H., Non-equilibrium ionization effects on the density line ratio diagnostics of O IV, *ApJ*, 767, 43, 2013.
- Pagano, I., Linsky, J. L., Carkner, L., et al., HST/STIS Echelle Spectra of the DM1E star AU microscopii outside of Flares, *ApJ*, 532, 497-513, 2000.
- Kramida, A., Ralchenko, Yu., Reader, J., and NIST ASD Team (2012). NIST Atomic Spectra Database (ver. 5.0), [Online]. Available: <http://physics.nist.gov/asd> [2013, June 6]. National Institute of Standards and Technology, Gaithersburg, MD.

Redfield, S., Linsky, J. L., Ake, T. B., et al., A far ultraviolet spectroscopic explorer survey of Late-type Dwarf stars, *ApJ*, 581, 626-653, 2002.

Sahal-Bréchet S., 1969, Impact theory of the broadening and shift of spectral lines due to electrons and ions in a plasma (continued), *A&A*, 2, 322-354, 1969.

Sahal-Bréchet, S., Dimitrijević, M. S., Moreau N., 2012, Stark-B database, [online]. Available: <http://stark-b.obspm.fr> [June 6, 2013]. Observatory of Paris, LERMA and Astronomical Observatory of Belgrade

Seaton, M., The Impact Parameter Method for Electron Excitation of Optically Allowed Atomic Transitions, *Proc. Phys. Soc.*, 79, 1105-1117, 1962.

Sturm, E., Lutz, D., Verma, A., et al., Mid-infrared line diagnostics of active galaxies, *A&A*, 393, 821-841, 2002.

Tayal, S. S., Breit-Pauli R-matrix calculation for electron collision rates in O IV, *ApJS*, 166, 634-649, 2006.

Table 1: Comparison of our present calculation of energy levels ($E_{Present}$) with those of NIST (Kramida et al., 2012), GRASP2 (Aggarwal and Keenan, 2008) (using 219 levels) and MCHF (Tayal, 2006). Energies are in Ry.

Index	Configuration	Level	J	$E_{Present}$	E_{NIST}	E_{GRASP2}	E_{MCHF}
1	2s ² 2p (¹ S)	² P ^o	0.5	0.00000	0.00000	0.00000	0.00000
2	2s ² 2p (¹ S)	² P ^o	1.5	0.00347	0.00352	0.00339	0.00337
3	2s 2p 3s (³ P ^o)	⁴ P	0.5	0.64455	0.65101	0.61591	0.65294
4	2s 2p 3s (³ P ^o)	⁴ P	1.5	0.64573	0.65220	0.61705	0.65405
5	2s 2p 3s (³ P ^o)	⁴ P	2.5	0.64767	0.65388	0.61860	0.65590
6	2s 2p 3s (¹ D)	² D	1.5	1.18155	1.15686	1.20775	1.17885
7	2s 2p 3s (¹ D)	² D	2.5	1.18156	1.15673	1.20760	1.17890
8	2s 2p 3s (¹ S)	² S	0.5	1.48399	1.49782	1.56308	1.53836
9	2s 2p 3s (³ P ^o)	² P	0.5	1.68195	1.64466	1.73160	1.68077
10	2s 2p 3s (³ P ^o)	² P	1.5	1.68427	1.64688	1.73369	1.68289
11	2p 3 (² S)	⁴ S ^o	1.5	2.11438	2.10993	2.11408	2.11881
12	2s ² 3d (¹ S)	² D	1.5	3.96459	3.82307	3.75789	3.83720
13	2s ² 3d (¹ S)	² D	2.5	3.96473	3.82323	3.75803	3.83706
14	2s 2p 3s (³ P ^o)	⁴ P ^o	0.5	3.98893	3.99909	3.92915	4.00397
15	2s 2p 3s (³ P ^o)	⁴ P ^o	1.5	3.99027	4.00032	3.93038	4.00509
16	2s 2p 3s (³ P ^o)	⁴ P ^o	2.5	3.99253	4.00257	3.93261	4.00712
17	2s 2p 3s (³ P ^o)	² P ^o	0.5	4.14723	4.12628	4.07957	4.14202
18	2s 2p 3s (³ P ^o)	² P ^o	1.5	4.14973	4.12869	4.08194	4.14239
19	2s 2p 3p (³ P ^o)	⁴ D	0.5	4.24800	4.26780	4.20150	4.27826
20	2s 2p 3p (³ P ^o)	⁴ D	1.5	4.24881	4.26851	4.20218	4.27890
21	2s 2p 3p (³ P ^o)	⁴ D	2.5	4.25016	4.26975	4.20336	4.28001
22	2s 2p 3p (³ P ^o)	⁴ D	3.5	4.25203	4.27166	4.20526	4.28170
23	2s 2p 3p (³ P ^o)	⁴ S	1.5	4.28655	4.32376	4.25326	4.33524
24	2s 2p 3p (³ P ^o)	² P	0.5	4.28710	4.25771	4.19583	4.26653
25	2s 2p 3p (³ P ^o)	² P	1.5	4.28871	4.25876	4.19691	4.26749
26	2s 2p 3p (³ P ^o)	⁴ P	0.5	4.36958	4.36359	4.29685	4.37240
27	2s 2p 3p (³ P ^o)	⁴ P	1.5	4.37041	4.36445	4.29769	4.37323
28	2s 2p 3p (³ P ^o)	⁴ P	2.5	4.37171	4.36563	4.29882	4.37433
29	2s 2p 3p (³ P ^o)	² D	1.5	4.41583	4.39838	4.35552	4.41476
30	2s 2p 3p (³ P ^o)	² D	2.5	4.41823	4.40071	4.35784	4.41681
31	2s 2p 3p (³ P ^o)	² S	0.5	4.49337	4.49155	4.46991	4.52115
32	2s 2p 3d (³ P ^o)	⁴ F ^o	1.5	4.50466	4.51231	4.45181	4.52369
33	2s 2p 3d (³ P ^o)	⁴ F ^o	2.5	4.50543	4.51302	4.45249	4.52369
34	2s 2p 3d (³ P ^o)	⁴ F ^o	3.5	4.50653	4.51405	4.45351	4.52461
35	2s 2p 3d (³ P ^o)	⁴ F ^o	4.5	4.50797	4.51545	4.45491	4.52588
36	2s 2p 3d (³ P ^o)	⁴ D ^o	0.5	4.54548	4.55421	4.48131	4.56333
37	2s 2p 3d (³ P ^o)	⁴ D ^o	1.5	4.54570	4.55447	4.48558	4.56358
38	2s 2p 3d (³ P ^o)	⁴ D ^o	2.5	4.54611	4.55490	4.48600	4.56397
39	2s 2p 3d (³ P ^o)	⁴ D ^o	3.5	4.54676	4.55549	4.48659	4.56451
40	2s 2p 3d (³ P ^o)	² D ^o	2.5	4.56950	4.57059	4.51958	4.58579
41	2s 2p 3d (³ P ^o)	² D ^o	1.5	4.56955	4.57009	4.51932	4.58533
42	2s 2p 3d (³ P ^o)	⁴ P ^o	2.5	4.57124	4.59366	4.52245	4.60176
43	2s 2p 3d (³ P ^o)	⁴ P ^o	1.5	4.57164	4.59469	4.52326	4.60268
44	2s 2p 3d (³ P ^o)	⁴ P ^o	0.5	4.57219	4.59536	4.52390	4.60329
45	2s 2 4s (¹ S)	² S	0.5	4.59636	4.42713	4.34934	4.41291
46	2s 2p 3d (³ P ^o)	² F ^o	2.5	4.64907	4.65425	4.61403	
47	2s 2p 3d (³ P ^o)	² F ^o	3.5	4.65133	4.65637	4.61622	
48	2s 2p 3d (³ P ^o)	² P ^o	1.5	4.67580	4.68592	4.64811	
49	2s 2p 3d (³ P ^o)	² P ^o	0.5	4.67709	4.68730	4.64954	4.56333
50	2s ² 4p (¹ S)	² P ^o	0.5	4.71223	4.55629	4.48532	
51	2s ² 4p (¹ S)	² P ^o	1.5	4.71258	4.55668	4.48168	4.56407
52	2s 2p 3s (¹ P ^o)	² P ^o	0.5	4.78493	4.72673	4.75301	
53	2s 2p 3s (¹ P ^o)	² P ^o	1.5	4.78501	4.72682	4.75313	
54	2s ² 4d (¹ S)	² D	1.5	4.81167	4.65265	4.57274	
55	2s ² 4d (¹ S)	² D	2.5	4.81171	4.65269	4.57279	
56	2s ² 4f (¹ S)	² F ^o	2.5	4.82628	4.67651	4.59047	
57	2s ² 4f (¹ S)	² F ^o	3.5	4.82631	4.67661	4.59051	
58	2s 2p 3p (¹ P ^o)	² D	1.5	5.04651	4.98760	5.03332	
59	2s 2p 3p (¹ P ^o)	² D	2.5	5.04675	4.98787	5.03353	
60	2s 2p 3p (¹ P ^o)	² P	0.5	5.07598	5.01007	5.03586	
61	2s 2p 3p (¹ P ^o)	² P	1.5	5.07660	5.01065	5.03645	
62	2s 2p 3p (¹ P ^o)	² S	0.5	5.14024	5.05265	5.11693	
63	2s 2p 3d (¹ P ^o)	² D ^o	1.5	5.28047	5.24725	5.30203	
64	2s 2p 3d (¹ P ^o)	² D ^o	2.5	5.28067	5.24756	5.30232	
65	2s 2p 3d (¹ P ^o)	² F ^o	3.5	5.29185	5.20148	5.27744	
66	2s 2p 3d (¹ P ^o)	² F ^o	2.5	5.29194	5.20143	5.27749	
67	2s 2p 3d (¹ P ^o)	² P ^o	0.5	5.35379	5.30103	5.35907	
68	2s 2p 3d (¹ P ^o)	² P ^o	1.5	5.35391	5.30123	5.35929	

Table 2: Comparison of our values of $\log(g_i f_{ij})$ and transition probability $A_{ji}(\text{s}^{-1})$ with the values of Galavís, Mendoza and Zeippen (1998), Flower and Nussbaumer (1975) and Tayal (2006) for 5 intercombination transitions. Observed wavelengths are from Bromander (1969).

Index	Transition	wav (Å)	Conf _i	J _i	Conf _f	J _f	log(gf)	A(s ⁻¹)	A(Galavis)	A(Flower)	A(Tayal)
1	1 – 4	1397.2	2s ² 2p ² P ^o	0.5	2s 2p ² ⁴ P	1.5	-7.316	40.69	48.36	58.2	36.6
2	1 – 3	1399.77	2s ² 2p ² P ^o	0.5	2s 2p ² ⁴ P	0.5	-5.98	1757.58	1724	2080	1280
3	2 – 5	1401.16	2s ² 2p ² P ^o	1.5	2s 2p ² ⁴ P	2.5	-5.688	1146.37	1331	1470	1025
4	2 – 4	1404.81	2s ² 2p ² P ^o	1.5	2s 2p ² ⁴ P	1.5	-6.347	374.79	314.7	441	251.3
5	2 – 3	1407.39	2s ² 2p ² P ^o	1.5	2s 2p ² ⁴ P	0.5	-5.973	1766.95	1762	2130	1264

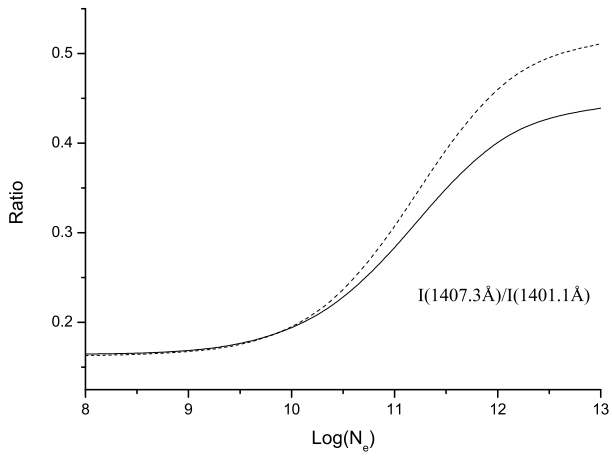


Figure 1: Our calculations: line ratio $I(1407.3 \text{ \AA})/I(1401.1 \text{ \AA})$ plotted as a function of logarithmic electron density (N_e in cm^{-3}) and at a constant electron temperature of $T_e=10^5$ K. The solid curve is obtained by using the oscillator strengths from [Galavis, Mendoza and Zeippen \(1998\)](#), and the dashed curve is obtained by using our HFR calculations for the 5 intercombination transitions.